Design Study of CANGAROO-III, Stereoscopic Imaging Atmospheric Cherenkov Telescopes for sub-TeV Gamma-ray Detection [⋆]

R. Enomoto [a,1], S. Hara [b,2], A. Asahara [b], G.V. Bicknell [c],
P.G. Edwards [e], S. Gunji [f], T. Hara [h], J. Jimbo [j], F. Kajino [i],
H. Katagiri [a], J. Kataoka [k], A. Kawachi [a], T. Kifune [a], H. Kubo [k],
J. Kushida [k], Y. Matsubara [ℓ], Y. Mizumoto [m], M. Mori [a],
M. Moriya [b], H. Muraishi [n], Y. Muraki [ℓ], T. Naito [h], T. Nakase [j],
K. Nishijima [j], K. Okumura [a], J.R. Patterson [d], K. Sakurazawa [b],
D.L. Swaby [d], K. Takano [b], T. Tanimori [k], T. Tamura [o],
K. Tsuchiya [a], K. Uruma [j], S. Yanagita [g], T. Yoshida [g],
T. Yoshikoshi [p], A. Yuki [ℓ]

[a]*ICRR, Univ. of Tokyo, 5-1-5 Kashiwa-no-ha, Chiba 277-8582, Japan*

[b]*Tokyo Inst. of Tech., Meguro-ku, Tokyo 152-8551, Japan*

[c]*Australian National University, ACT 2611, Australia*

[d]*Dept. of Phys. and Math. Phys., Univ. Adelaide, SA 5005, Australia*

[e]*ISAS, Sagamihara, Kanagawa 229-8510, Japan*

[f]*Dept. Phys., Yamagata Univ., Yamagata, Yamagata 990-8560, Japan*

[g]*Ibaraki University, Mito, Ibaraki 310-8512, Japan*

[h]*Yamanashi Gakuin University, Kofu, Yamanashi 400-8575, Japan*

[i]*Dept. of Phys., Konan University, Kobe, Hyogo 658-8501, Japan*

[j]*Tokai University, Hiratsuka, Kanagawa 259-1292, Japan*

[k]*Dept. of Phys., Kyoto University, Sakyo-ku, Kyoto 606-8502, Japan*

[ℓ]*STE Lab., Nagoya University, Nagoya, Aichi 464-8602, Japan*

[m]*National Astronomical Observatory, Mitaka, Tokyo 181-8588, Japan*

[n]*IPU, Ami, Ibaraki 300-0394, Japan*

[o]*Kanagawa University, Yokohama, Kanagawa 221-8686, Japan*

[p]*Dept. of Phys., OCU, Osaka, Osaka 558-8585, Japan*

Abstract

CANGAROO-III is an Imaging Atmospheric Cherenkov Telescope (IACT) array of four 10 m telescopes for very high energy (sub-TeV) gamma-ray astronomy. A design study of

the CANGAROO-III telescope system was carried out using the Monte Carlo technique in order to optimize the pixel size and the telescope spacing. Studies were also made of observations at low elevation angles.

1 Introduction

CANGAROO-III is an Imaging Atmospheric Cherenkov Telescope (IACT) array observing very high-energy (sub-TeV) gamma-rays from the universe. The four 10 m diameter telescopes can operate independently or as an array.

The CANGAROO experiment is located in Woomera, South Australia. It started from a 3.8-m telescope[1] (CANGAROO-I) in 1992. The second stage, CANGAROO-II, commenced in 1999 with the construction of a 10 m telescope mount with a mirror initially of 7 m diameter. The mirror was extended to 10 m in 2000 [2]. CANGAROO-III will be an array of four telescopes, with the existing CANGAROO-II telescope being the first of these.

We studied the basic design parameters for the next three telescopes using the Monte Carlo technique. Similar studies have been carried out previously, for example by the VERITAS [3] and HESS [4] groups. We started from optimized parameters obtained by a previous study and our experience with CANGAROO-I,[1] and verified those results. The pixel size and the telescope spacing were optimized. Also, some studies concerning the geomagnetic field effects and the possibility of large zenith angle observations were included.

2 Monte Carlo

Electromagnetic and hadronic shower simulations in the air using a Monte-Carlo code were conducted based on GEANT3.21 [5]. In this method, the atmosphere is divided into 80 layers of equal thickness ($\sim 12.9 g/cm^2$). Each layer corresponds to less than a half radiation length. The dependence of results on the number of layers was checked by halving the number of layers and was confirmed to be less than a 10% effect. The lower energy threshold for particle transport was set at 20 MeV,

Table 1
Main parameters of CANGAROO-II telescope.

parameters	values
coordinate	136°E, 31°S
height above sea level	220m
total diameter	10m
focal length	8m
number of mirror-segmentation	114
mirror radius	80cm
mirror shape	spherical
mirror alignment	parabolic
mirror curvature	16.4m
mirror material	plastic

which is less than the Cherenkov threshold of electrons at normal temperature and pressure (NTP). Most Cherenkov light is emitted higher in the atmosphere, i.e., at less pressure and a higher Cherenkov threshold. The geomagnetic field at the Woomera site (South Australia) was included in the simulations (0.253 gauss in horizontal and 0.520 gauss in vertical directions, and 6.8° degrees off from south).

In order to save CPU time, Cherenkov light was tracked in the simulations only when it was initially directed to the mirror area. The average mirror reflectivity and the measured photo-multiplier (PMT) quantum efficiency were multiplied by the Frank-Tamm equation to derive the total amount of light and its wavelength dependence. A Rayleigh-scattering length of $2970(\lambda/400nm)^4 \ [g/cm^2]$ was used in transport to the ground [6]. No Mie scattering was assumed in this study. The contribution of Mie scattering is thought to be at the 10–20% level, and we therefore consider this study to have uncertainties at at least this level. When Rayleigh scattering occurred, we treated it as absorption. The diameter of each spherical mirror segment is 80 cm. We assumed a perfect spherical shape (i.e., no deformation and no blur spot) with the CANGAROO-II geometry [7]. The main telescope parameters are listed in Table 1. The average measured reflectivity of 80% at 400 nm was adopted. The curvature of the mirror segments is 16.4 m. In total, 114 mirrors were aligned in a parabolic shape with a focal length of 8 m.[7]

For the simulations, we tried the use of four different camera designs:

setup 1: Five hundred and seventy-six 1/2″ PMTs of the same type as the CANGAROO-II camera [2]. With a pixel spacing of 0.112°, the total field of view (FOV) was 2.7° × 2.7° square.
setup 2: Five hundred and seventy-six 3/4″ PMTs. A pixel spacing of 0.168° yields

a FOV of 4° square.

setup 3: Two hundred and fifty-six 3/4″ PMTs, with a FOV of 2.7° square.

setup 4: Five hundred and seventy-six 3/4″ PMTs with a smaller PMT separation than in setup 2: a pixel spacing of 0.147° and a FOV of 3.5°.

The shape of the photocathodes was assumed to be circular. Each PMT had a light guide above the surface of the photo-cathode. The gain in light yield was assumed to be 1.6 compared to the case without it.[2]

In order to simulate cosmic-ray background events, we generated only protons with a differential energy spectrum of $E^{-2.7}$. The minimum and maximum energies of the generated range were 100 and 5000 GeV, respectively, in the case of zenith injection. For the large zenith angle study, we increased the maximum energy to 20 TeV. The maximum core distance of simulated showers was 300 m in radius for the zenith injection. We also increased it for the large angle injection. For example, we used 1000 m for 55° injection. The maximum offset angle for cosmic-ray showers was 5 degrees. We generated typically 100,000 events for each setup.

For gamma-ray cascades, we chose $E^{-2.5}$ spectrum (Crab-like spectrum [11]). The minimum and maximum of the generated energies were 50 and 5000 GeV, respectively, for cascades from the zenith, with the maximum increased for the low elevation simulations.

Finally, electronics noise was added and the timing responses were smeared using Gaussian of 4 nsec (σ). We also added Night Sky Background (NSB) photons, conservatively selecting to double Jelley's value of $2.55 \times 10^{-4} erg/cm^2/sec/sr$ (430-550 nm) [8].

3 Analysis

First, we applied a threshold for the PMT pulse-heights. The threshold was set at 5 photoelectrons. This greatly reduced the effect of NSB photons. Second, we applied a clustering cut. Only PMTs exceeding the threshold ("hits") and having more than two adjacent hits were selected (t3a clustering[3]). A hit map of an event is shown in Figure 1.

The left figures are for telescope-1 and the right are for telescope-2. The spacing of the telescopes was 100 m. The box sizes are proportional to the number of photoelectrons. The upper figures were obtained without this clustering and the lower ones used this clustering cut. Isolated pixels triggered by NSB photons were all removed by this operation.

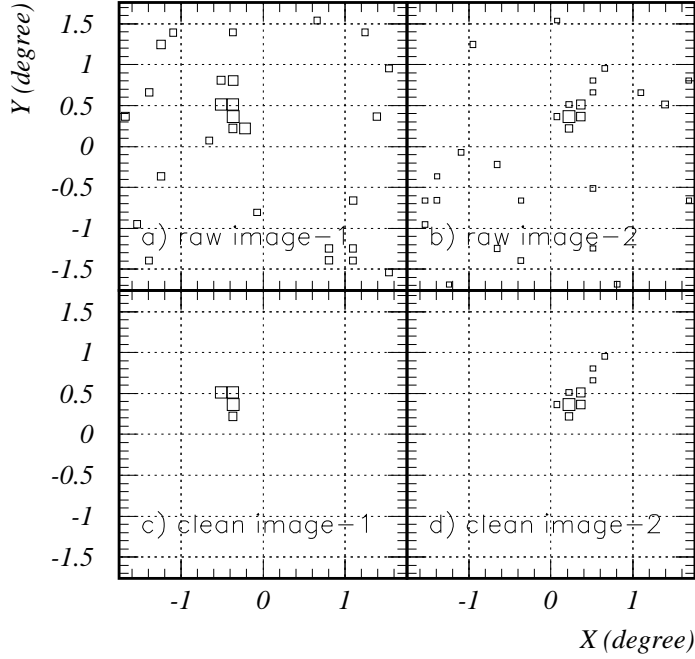The selection of gamma-ray events was carried out using the standard imaging

4

Fig. 1. *Simulated camera images for two telescopes separated by 100 m. The box sizes are proportional to the number of photo-electrons. a) raw image of telescope 1, b) raw image of telescope 2, c) cleaned image of telescope 1, and d) cleaned image of telescope 2.*

analysis technique. The imaging analysis was based on parameterization of the Cherenkov light image by its "width," "length," "conc" (shape), "distance" (location), and the image orientation angle (α) [9]. The energy dependence of some parameters is shown in Figure 2. For example, "length" has a linear correlation with the logarithm of energy. We, therefore, used a linearly corrected "length" instead of the original one. We applied similar corrections to the other parameters.

Using these parameters, except for α, we carried out a likelihood analysis in order to separate gamma-ray–like showers from hadron-like showers [10]. In order to make a probability density function (PDF), we generated two kinds of Monte Carlo event samples. The gamma-ray sample was made assuming the primary flux to be proportional to $E^{-2.5}$ (the spectrum of the Crab pulsar [11]). The hadron sample assumed a spectrum of $E^{-2.7}$. Using these two samples, we made PDFs from histograms of the shower parameters. We calculated the probability on an event-by-event basis of the event being due to a gamma-ray using

$$Prob = \Pi\{Prob(i, \gamma)/(Prob(i, \gamma) + Prob(i, p))\},$$

where the suffix i refers to the shower parameters. A cut was subjected to the parameter χ^2s, which is $-2\ln(Prob)$, as shown in Figure 3. The smaller χ^2 events
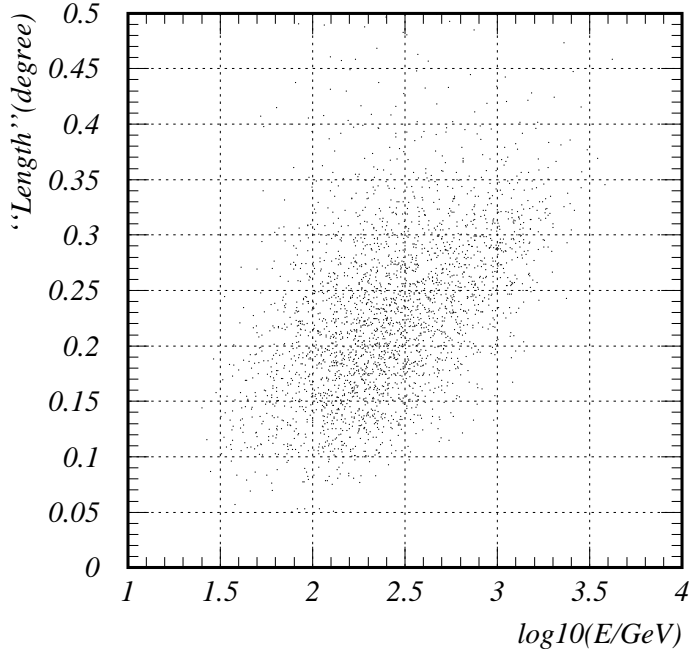
5

Fig. 2. *Energy dependence of the "length" parameter, i.e., the "length" versus the detected number of photo-electrons.*

are likely to be gamma-ray events. The blank histograms are for gamma-ray events and the hatched one for hadrons. The left hand figure is for a single-telescope analysis, and the right one is for a stereo (two telescope) analysis. In analyzing the stereo case, the probability was calculated by $Prob(telescope - 1) \times Prob(telescope - 2)$. The signal-to-noise ratios (S/N) were greatly improved by stereoscopic observations while maintaining shower detection efficiency when both telescopes have analyzable images.

4 Pixel Size

The present pixel spacing of the CANGAROO-II camera is $0.112°$ [2]. This is based on the use of $1/2''$ PMTs and is the setup 1 described previously. This setup has a FOV of $2.7°$ square. With this FOV, we are forced to conduct so-called "Long ON/OFF" mode for observations [12]. For example, a 3 hr "ON" source observation and a 3 hr "OFF" source observation may be made during one night. This operation reduces the observation period significantly — by a factor of two. In order to carry out ON and OFF source observations simultaneously, we need a FOV of approximately $4°$. As the major part of shower images for gamma-rays are typically con-
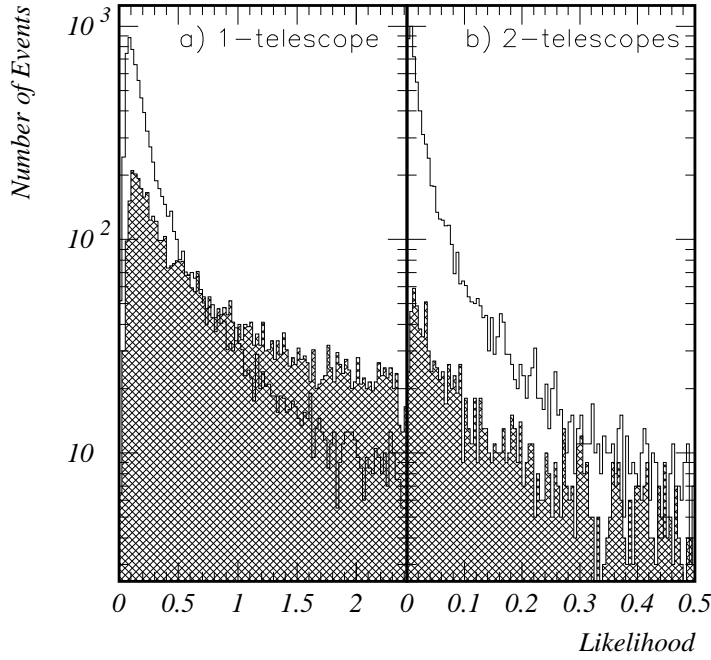
6

Fig. 3. *Log-Likelihood distribution, i.e., χ^2. The blank histograms are for gamma-rays and the hatched areas are protons; a) for 1 telescope, and b) for 2 telescopes (in stereo mode).*
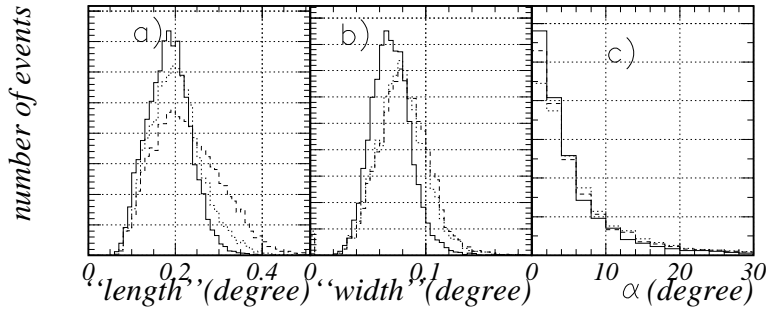

Fig. 4. *Comparison of parameters (a) length, (b) width, and (c) α for three camera designs. The curves are for gamma-rays. The solid lines are for setup 1, the dashed lines are setup 2, and the dotted lines are setup 3.*

tained within a $1°$ circle, we investigated the use of setup 2, with a larger PMT size ($3/4''$ circular photocathode). Because of the weight limitation due to the telescope structure, we can not increase the camera weight very much [7]. We compared the shower image parameters for both cases, as shown in Figure 4. The deterioration of α resolution is very small, as shown in Figure 4c). The width deteriorates slightly
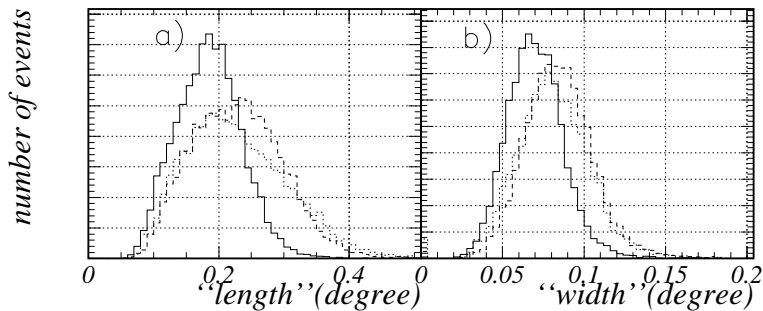
7

Fig. 5. *Comparisons between setup 4 and setups 1 and 2 for (a) length, and (b) width: The solid line is setup 1, the dotted setup 2, and the dashed setup 4. The curves are for gamma-rays.*

due to the pixel-size effect, but not that greatly (Figure 4b). The length, however, changed significantly (Figure 4a). In order to check the FOV effect, we tried setup 3, i.e., the same PMT size as setup 2 but the same FOV as setup 1. From Figure 4a it is apparent that the deterioration in length is due to the change in the FOV. We conclude that the smaller FOV deforms the length distribution and that setup 2 is preferred.

A $3/4''$ PMT has a diameter of 18.6 ± 0.7 mm[13]. In setup 2, the spacing of the PMTs was 24 mm. A clearance of 5 mm was kept. We tried setup 4 with a spacing of 21 mm (clearance of 2 mm). Comparisons in Figure 5 show that the difference is sufficiently small. We again concluded that the setup 2 is a reasonable choice. In the real design of the CANGAROO-III camera, we have selected a "hexagonal" arrangement of PMTs with alternate rows offset by half a pixel.

5 Telescope Spacing

5.1 Stereo Mode

With a likelihood analysis and the above-mentioned camera design ("setup-2"), we proceeded to design a stereoscopic telescope system. Previous studies have investigated the effect of the telescope spacing [3][4]. These indicated that a spacing within a range of 80 to 120 m is best. We, therefore, tested the range between 60 and 140 m. Here, we assumed two telescopes. We started from calculations of "effective area" versus the incident gamma-ray energy. Gamma-rays of various energies from the zenith were generated. The results are shown in Figure 6. Here, the effective area is the product of the "real" effective area (m^2) and the Crab-like spectrum $(E/GeV)^{-2.5}$ in order to show the effective threshold. Those curves were obtained
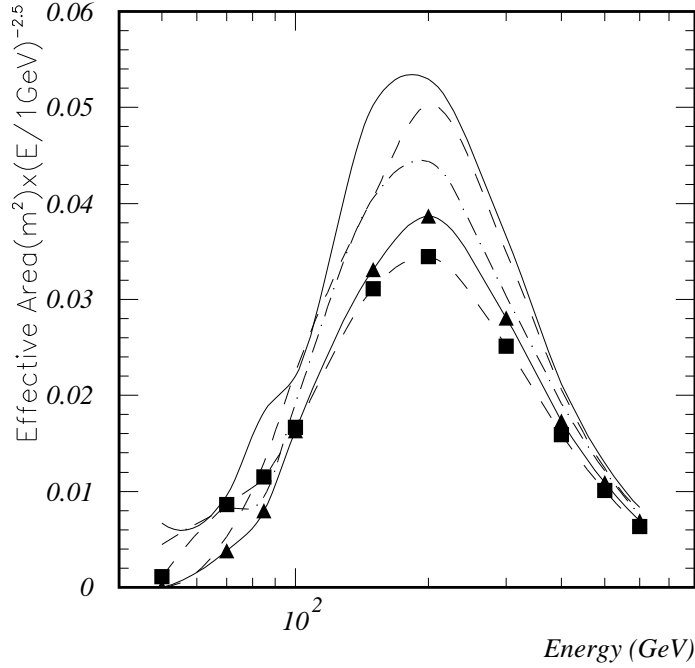
8

Fig. 6. *"Effective area" versus the incident γ-ray energy. The vertical axis is the effective area (m^2) multiplied by the $(E/GeV)^{-2.5}$-energy spectrum. The telescope spacing was varied from 60 to 140 m; the solid line is for 60 m, the dashed 80 m, the dot-dashed 100 m, the solid with triangles 120 m, and the dashed with squares 140 m.*

after smoothing. They peak at around 200 GeV and are a decreasing function of the telescope spacing. The light pool on the surface has a radius of approximately 100 m. The coincidence rate of the two telescopes, therefore, decreases as the spacing increases.

In the stereoscopic mode, the images from the two telescopes should point to the same direction, i.e., to the source direction. The angular resolution of this method should improve with a larger telescope spacing due to the larger opening angles of images. This is shown in Figure 7. In the figure, the curves "wiggle" below 100 GeV due to the lack of Monte-Carlo statistics, but the general trend of worsening angular resolution with decreasing energy is clear. This has an opposite energy dependence compared with that of the effective area. Typically, at around the threshold (∼200 GeV), the angular resolution is 0.2° per shower.

For a point-source observation, we can define the following figure of merit (FOM) using the above two parameters:

$$FOM = \text{``}effective\ area\text{''}/\sqrt{angular\ resolution}[m^2 GeV^{-2.5}(degree)^{0.5}].$$

9
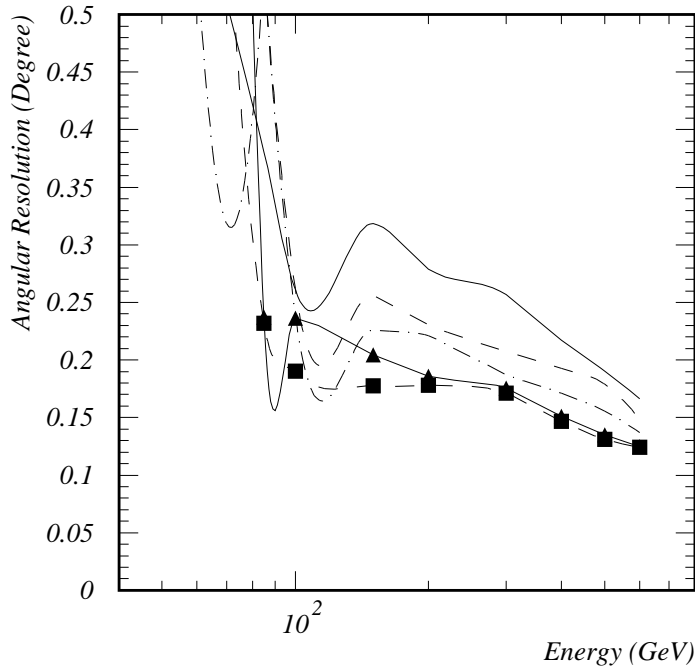
Fig. 7. *Angular resolution versus the incident γ-ray energy. The resolution is obtained on an event-by-event basis. The solid line is for 60 m, the dashed 80 m, the dot-dashed 100 m, the solid with triangles 120 m, and the dashed with squares 140 m.*

This value is proportional to the statistical significance of the observations. The energy dependence of the FOM for various telescope spacings are plotted in Figure 8. The FOM is maximized at the 80 m spacing. The dependency on the spacing, however, is small within this range. Also, the energy threshold for the stereoscopic mode was obtained to be 200 GeV. In conclusion, telescope spacings of between 60 and 140 m are all acceptable. We selected a 95–100 m spacing for the CANGAROO-III experiment.

5.2 Monocular Mode

We can operate multi-telescopes independently. We assumed that data from each telescope were recorded whenever it triggers, and that "stereo" triggering is done later in software analysis. We call this the "Monocular Mode". In this mode, when all telescopes have the same pointing direction, we expected a much improved effective area, especially at low energies. The calculated effective area for the monocular mode is shown in Figure 9. It was obtained under the trigger condition, in which one of two telescopes satisfies the analysis conditions. The gain in the ef-
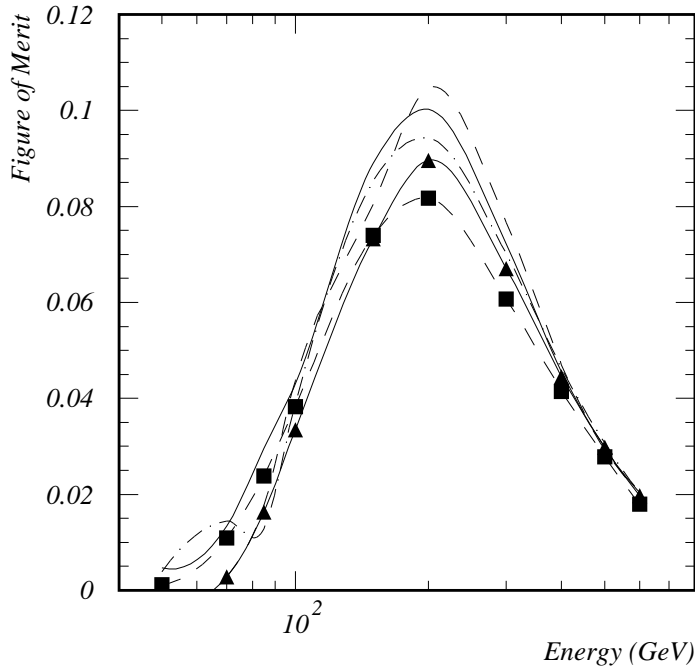
10

Fig. 8. *Figure of merit (described in the text) versus the incident γ-rays energy. The solid line is 60 m, the dashed 80 m, the dot-dashed 100 m, the solid line with triangles 120 m, and the dashed with squares 140 m.*

fective area at lower energies is very much improved. The energy threshold of this mode was obtained to be 100 GeV. We hope that this mode will work as a "discovery mode". At higher energies, such as 1 TeV, the effective areas for both the stereo and monocular modes coincide.

5.3 Large Angle Observation

It is well known that observations at large zenith angles (i.e., low elevation angles) are effective for higher energy measurements [11]. This is due to an increase in an effective area because of the inclined injection of gamma-rays to the atmosphere. For example, we show the light pool on the Earth's surface of a gamma-ray shower which is injected 55° inclined from the zenith (Figure 10 lower plot). The azimuthal direction of this injection is north-west. The camera of the setup-2 was used. Here, we also used an 80-layer atmosphere and the GEANT package. Gamma-rays from the zenith make light pools with the density peaking at a radius of 120 m. The light profile is enlarged by a factor of ~4, most notably in the longitudinal direction but also in the transverse direction. The upper plots are the focal-plane images of
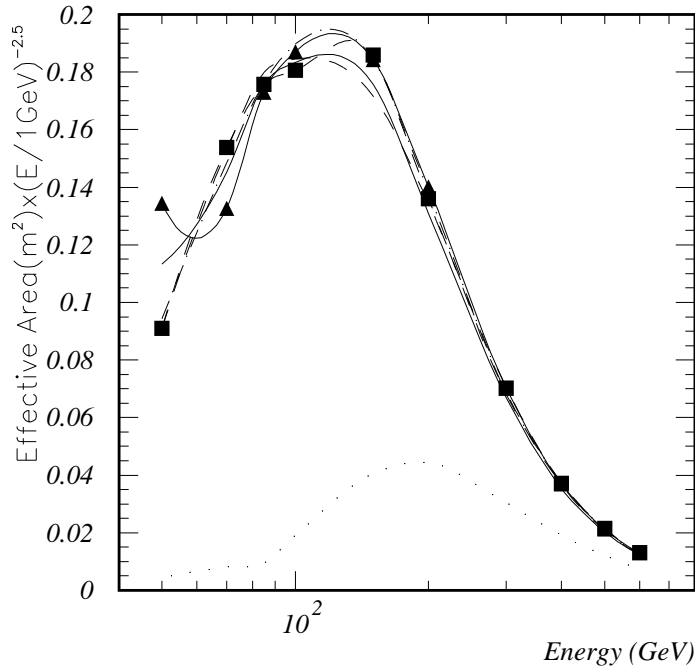
Fig. 9. *Total detection areas versus incident gamma-ray energy with "monocular mode",
i.e., by an independent two-telescope analysis. The solid line is 60 m, the dashed 80 m, the
dot-dashed 100 m, the solid line with triangles 120 m, and the dashed with squares 140 m.
The dotted line is the effective area obtained for the two-telescopes configuration (stereo
mode) with 100m separation.*

this shower. The drawback with this technique is that shower images shrink. The
gamma/hadron discrimination, therefore, using shower parameters, deteriorates, re-
ducing the S/N ratio and the α resolution is also worsened. Although the detection
possibility for low elevation observing was proved by CANGAROO-I in observa-
tions of the Crab [11], we can justify the use of this technique even for stereoscopic
modes. The differences in the shape parameter distributions are shown in Figure 11:
for distance, length, width, and α. The α distribution still has a peak, as shown in
Figure 11d. The other parameters also have differences between gamma-rays and
hadrons. Although the gamma-ray images shrink, the hadron images shrink in the
same way and it is still possible to discriminate between them.

In the case of a largely inclined shower, the geomagnetic effect becomes compara-
ble with the intrinsic shower-image size in the direction perpendicular to the mag-
netic field. In that direction, a deterioration of the angular resolution is expected
[14]. This means that a difference is introduced whether the telescopes are sepa-
rated east-west or north-south. The difference in the angular resolutions is shown
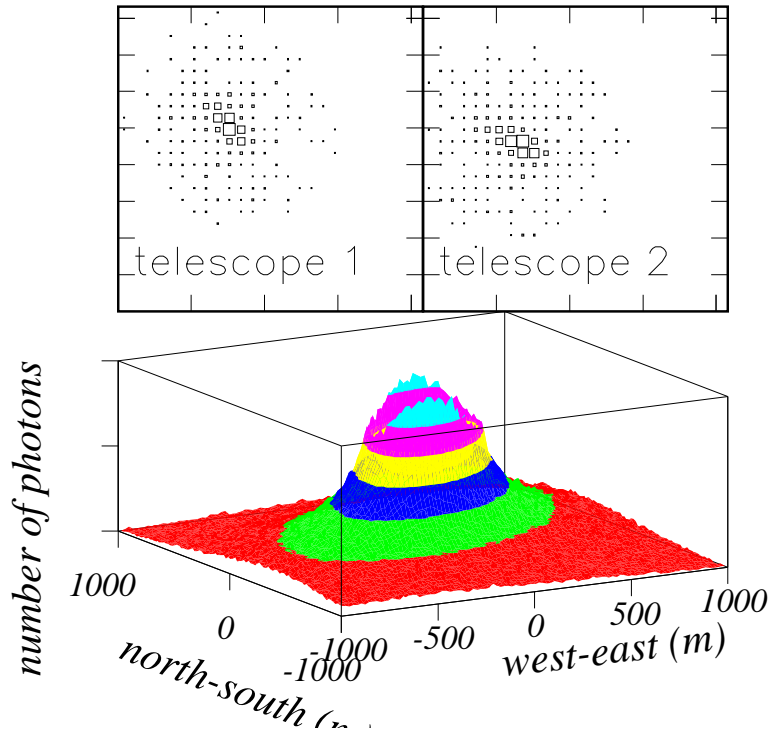in Figure 12. Clearly, an east-west setup is better than north-south. The second

12

Fig. 10. *Light pool of a large zenith angle event (lower plot). The scale is in meters. The upper plots are the focal-plane images for two telescopes.*

CANGAROO-III telescope will be built at a position 100 m West of the existing CANGAROO-II telescope.

Finally, we demonstrate the feasibility of the large zenith angle stereoscopic observations in the case of the east-west setup. The FOM is shown in Figure 13. Again, the spacings between 60 and 140 m are all acceptable. The FOM for the 100 m spacing is located near the maximum. The energy threshold of this mode at the zenith angle of $55°$ was obtained to be 700 GeV. At 700 GeV, the angular resolution obtained was $0.43°$ per shower. The effective area was $1.2 \times 10^5 m^2$ at 700 GeV.

6   Discussion

Considering the values obtained by this study, we determined the design of the second CANGAROO-III telescope. The location of the second telescope is 100 m west from the present CANGAROO-II telescope. The third and fourth telescopes will be located north and south from the baseline of the first two telescopes, i.e., at the corners of a diamond shape. The camera pixel spacing was determined to be $0.168°$ using 3/4″ PMTs. A hexagonal alignment was adopted. The total field
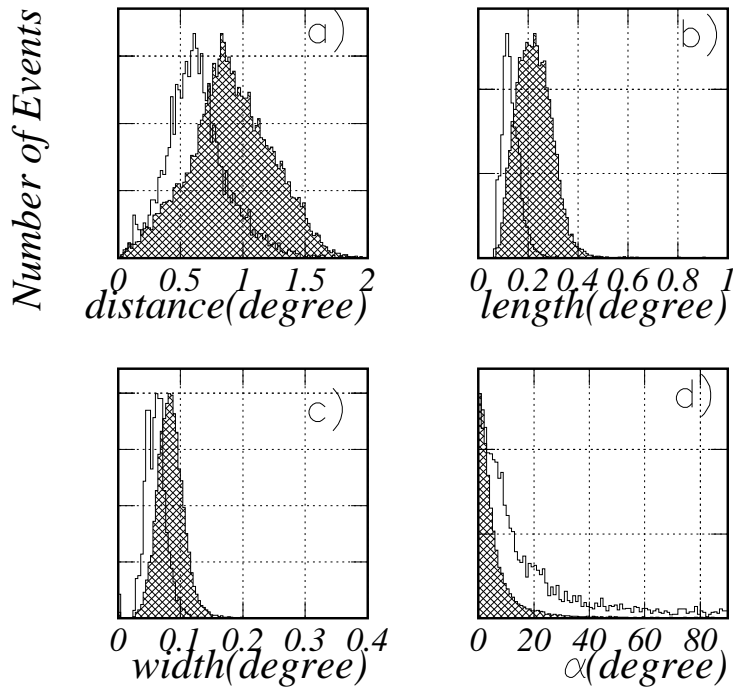
Fig. 11. *Comparisons of shower parameters: a) "distance", b) "length", c) "width", and d) α. The blank histograms were obtained by 55°-observations and the hatched ones by zenith observations. The shower parameters were shrunk due to the large distances between the telescope and the shower-max positions.*

of view is a hexagonal shape approximately 4° across. The second telescope is scheduled to be built in 2001.

7 Conclusion

A design study of the CANGAROO-III telescope system was carried out using the Monte Carlo technique. The optimized pixel spacing is 0.168° with use of 3/4 inch PMT's. This was carried out for gamma-rays from zenith positions. The telescope spacing for stereoscopic observations was optimized to be 100 m. The energy threshold at zenith was determined to be 200 GeV with an effective area of $2.4 \times 10^4 m^2$. The angular resolution per shower for stereo observations was 0.2° at 200 GeV, event by event bases. With this advantage, we can analyze profiles of the broad gamma-ray sources. For the monocular mode of the two-telescope system, the effective area was determined to be $1.8 \times 10^4 m^2$ with a threshold energy of 100 GeV. Low elevation observations, at a zenith angle of 55°, were investigated and an effective area of $1.2 \times 10^5 m^2$ with an energy threshold of 700 GeV
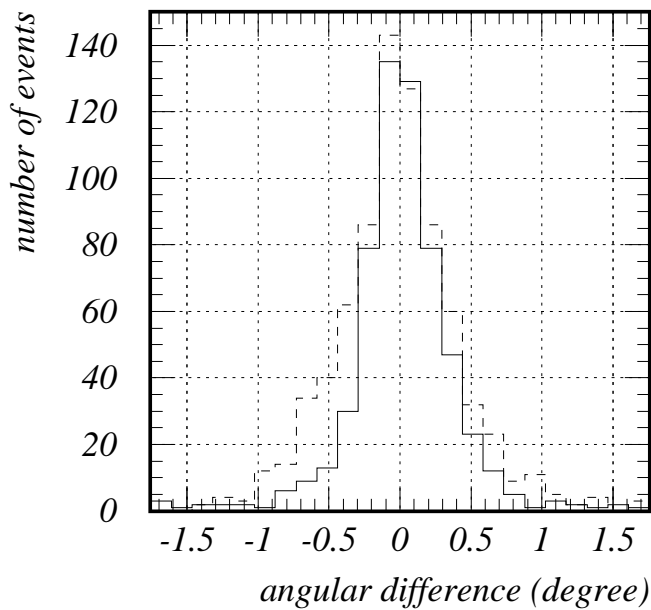
14

Fig. 12. *Angular difference between real and derived directions for large zenith-angle observations. The solid histogram was obtained from the north-south setup and the dashed histogram from the east-west setup.*

obtained. The angular resolution for stereo observations was $0.43°$ per shower at $700\,\mathrm{GeV}$. CANGAROO-III will be constructed using these design parameters.

Acknowledgement

References

[1] Hara, T. *et al*, Nucl. Instr. and Meth., A332 (1993) 300.

[2] Tanimori, T. *et al*, Proc. of 26th Int. Cosmic Ray Conf. (Utah) 5 (1999) 203; Kawachi, A. *et al*, ibid, 5 (1999) 207.

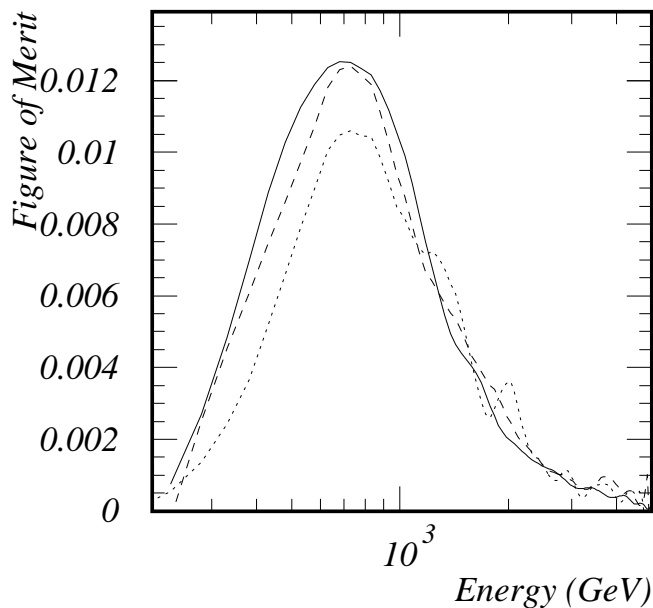[3] VERITAS proposal; http://veritas.sao.arizona.edu/.

Fig. 13. *Figure of merit versus the energies and spacings for large zenith angle, stereo mode observations. The solid line is for 60 m spacing, the dashed 100 m, and the dotted 140 m.*

[4] Hofmann, W. *et al*, Astropart. Phys. 13 (2000) 253.

[5] CERN Program Library Long Writeup W5013.

[6] Baum and Dunkelman, J. Opt. Soc. Am. 45 (1955) 166

[7] Kawachi, A. *et al*, Astropart. Phys. (in press).

[8] Jelley, J.V., "Cherenkov Radiation and its Applications", (Pergamon Press, 1958) p.219.

[9] Hillas, A.M., Proc. 19th Int. Cosmic-Ray Conf. (La Jolla), 3 (1985) 445; Weekes, T.C. *et al*, Astrophys. J. 342 (1989) 379.

[10] for example, Asner, D.M. *et al*, Phys. Rev. D53 (1996) 1039.

[11] Tanimori, T. et al., Astrophys. J. 429 (1994) L61; Tanimori, T. et al., Astrophys. J. Lett., 492 (1998) L33.

[12] Kifune, T. et al., Astrophys. J. 438 (1995) L91.

[13] Hamamatsu Photonics K. K., "Photomultiplier Tubes and Assemblies For Scintillation Counters and High Energy Physics".

[14] Chadwick, P.M. *et al*, Proc. of 26th Int. Cosmic Ray Conf., (Utah) 5 (1999) 231.